UDC 537.621.2:681.327.634

CPP Operational Mode of GMR Head

●Keiichi Nagasaka ●Yoshihiko Seyama ●Reiko Kondo
●Hirotaka Oshima ●Yutaka Shimizu ●Atsushi Tanaka

(Manuscript received September 14, 2001)

We have investigated the magneto-resistance (MR) properties of spin-valves (SVs) operating in the current perpendicular to plane (CPP) mode. These SVs are strong candidates for ultra-high-density recording heads because of their low resistance and high sensitivity. By adding an oxide layer to a CPP element consisting of a conventional single SV film, we changed its resistance-change area product ΔRA from 0.6 mΩμm² to 34 mΩμm² and its MR ratio from 0.5% to 2%. These dramatic changes may have been achieved because the oxide layer narrowed the current-flow area. Micromagnetics simulation revealed that a moderate-impedance CPP head such as an SV film with an oxide layer shows several advantages compared with low-impedance heads, for example, a higher output voltage and signal-to-noise ratio, less influence from the magnetic field of the sense current, and a narrower core width. We believe the CPP-SV head will play an important role in the read heads of future hard disk drives (HDDs).

1. Introduction

Ultra-high-density recording over 100 Gbit/in² requires a highly sensitive read head. To meet this requirement, the current perpendicular to plane (CPP) head is a stronger candidate than the modified current in plane (CIP) head, which has been used in recent hard disk drives (HDDs). The CPP is stronger because, if the power consumption in the sensor is made constant to avoid a temperature rise, the output voltage of the CPP head is roughly inversely proportional to the square root of the sensor area. The CPP head therefore provides a higher output voltage as the sensor size becomes smaller.

Figure 1 shows the target properties for 0.1 μm × 0.1 μm CPP elements of 100 Gbit/in² read heads. The area is estimated by considering the power consumption, electron migration of the element, and data transfer rate. A tunnel magneto-resistive (TMR) head is one of the candidates for realizing high sensitivity. However, it has several disadvantages, for example, it has a large resistance, which limits the operating frequency and makes the Johnson and Shot noise high, and it is too difficult to reduce its resistance without a breakthrough in fabrication technology for low-resistance barrier-layers.

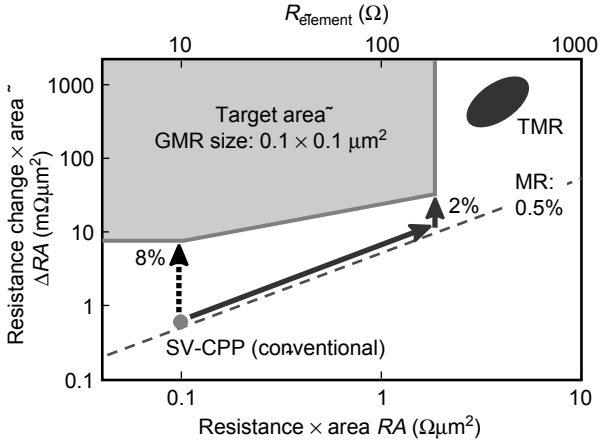

Figure 1
Target properties of sensor element for 100 Gbit/in² read head.

Another candidate is a CPP head using a giant magnetoresistive (GMR) film. Such a head has a much smaller impedance than a TMR head. Several researchers have studied GMR properties in the CPP mode both experimentally and theoretically because understanding them will help us to develop a comprehensive understanding of spin-dependent transport phenomena.[1)-6)] CPP heads using GMR multilayers have also been studied.[7),8)] Although multilayer CPP heads are expected to provide a large output signal, they have problems, for example, they generate hysteresis and the magnetic domains of their read element are difficult to control. Moreover, if we use in-gap type read heads for high-density recording, the sensor films must be thinner than the read gap. In contrast, the CPP heads that use a spin-valve (SV) film that have recently been used in HDDs do not have the problems associated with GMR multilayers.

In view of the above, the CPP-SV head (**Figure 2**) is a preferable structure for ultra-high-density recording. However, the MR ratio of a CPP element with a conventional SV is only about 0.5% and its output voltage, which is related to the resistance change, is too low. One way to realize the target properties is to increase the resistance change by optimizing the materials and layer structure, but this would be difficult because the MR ratio would need to be increased more than 16 times. On the other hand, if the element resistance is increased to the limit, its MR ratio only needs to be 2%, which is only four times larger than the 0.5% value of a conventional SV. We therefore decided to try to reach the target properties by increasing not only resistance change but also the element resistance.

In this study, we improved the MR properties of CPP-SV elements so they can be used for 100 Gbit/in^2 recording. The improvements were achieved by optimizing the SV structure to increase the resistance change and by using an oxide layer to control the resistance. We also investigated the read-back performance of a 0.1 μm × 0.1 μm CPP-SV head using micromagnetics simulation to investigate the feasibility of using CPP-SV heads.

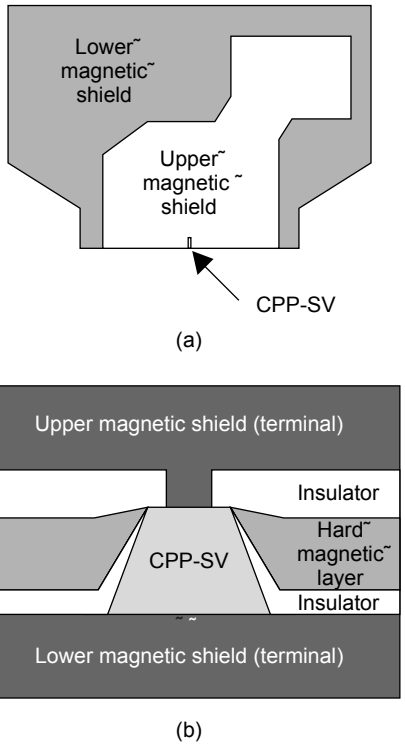

Figure 2
Schematic diagram of (a) top view and (b) cross section of a conventional CPP-SV head.

2. GMR properties in the CPP mode of SV films

2.1 Sample preparations

Figure 3 shows a schematic plane view of a

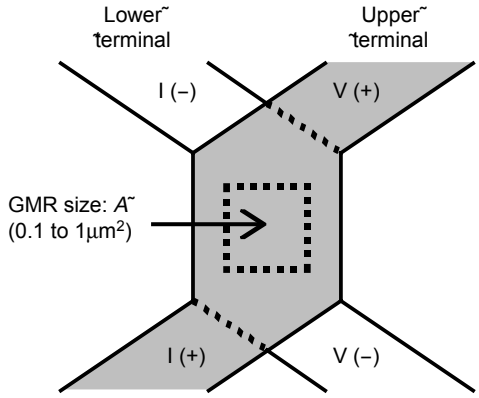

Figure 3
Schematic plane view of the CPP element.

CPP element, and **Figure 4** shows a cross-sectional image of a CPP element we fabricated. The element has two current terminals and two voltage terminals. The element has a SV film deposited on Al_2O_3TiC/Al_2O_3 substrates with a lower terminal layer having a sheet resistance R_S of about 40 mΩ. The details of the fabrication process are given elsewhere.[9] A capping layer of Cu was sequentially deposited on the SV film. An Au layer was also deposited using another sputtering machine to obtain a low contact resistance with the upper terminal. The SV film was ion-milled followed by lift-off processing of the insulator layer. Because the size was reduced, the GMR pillar became cylindrical due to the limitation of photolithographic resolution. Finally, an upper-terminal layer of Cu was deposited and patterned.

2.2 Conventional SV films in the CPP mode

2.2.1 Single SV films

A bottom-type single SV film with a Ta/NiFe /PdPtMn (15)/CoFeB (1.5)/Ru (0.8)/CoFeB (2.5)/ Cu (2.8)/CoFeB (2)/Ta (5) structure was used (the numerical values in parentheses denote the thickness [nm] of each layer). **Figure 5** shows the resistance R and resistance change ΔR as a function of the GMR size A of the CPP elements. The measuring current was kept below 5 mA so that its magnetic field did not affect the operation. R and ΔR were both proportional to $1/A$.

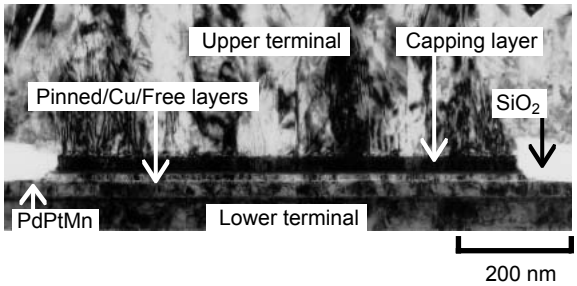

Figure 4
Cross-sectional view of CPP element.

The resistance-area product RA was 100 mΩμm^2, and the resistance change-area product ΔRA was 0.59 mΩμm^2. The MR ratio of the element was 0.59%. The measured R includes the terminal and contact resistances, which we collectively refer to as the parasitic resistance R_{para}. The RA of the SV $R_{sv}A$ is roughly calculated from the resistivity in the CIP mode and the thickness of each layer to be about 52 mΩμm^2. Therefore, the $R_{para}A$ was estimated to be 48 mΩμm^2.

2.2.2 Thicker magnetic layers and dual-structure SV films

Another SV film with thicker magnetic layers having the structure Ta/NiFe/ PdPtMn (15)/ CoFeB (4)/Ru (0.8)/CoFeB (5)/Cu (5)/CoFeB (3.5)/ Ta (5) was studied to examine the effects of bulk scattering. We then investigated the properties of dual-structure SV films.

Whereas a single SV film has only two interfaces between the magnetic and non-magnetic layers, a dual-structure SV has four such interfaces. As a result, when it is in the CIP mode, it exhibits a higher resistance change due to its higher interfacial scattering.[10] We therefore also studied the CPP properties of SV films having the

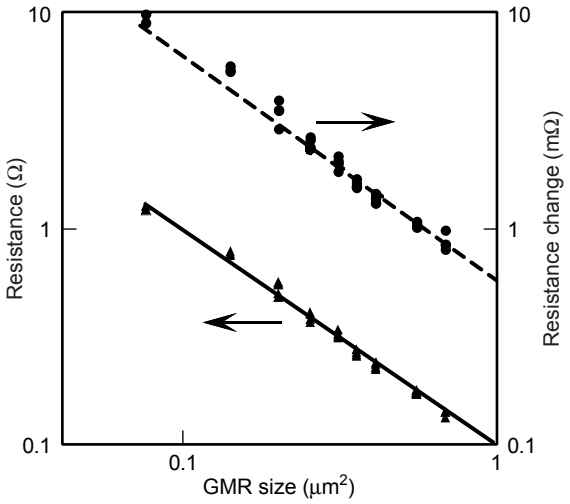

Figure 5
Resistance R and resistance change ΔR of the element as a function of GMR size A.
Solid and dashed lines are the fitting lines for $R = 0.1/A$ (Ω) and $\Delta R = 0.59/A$ (mΩ).

following dual structures: 1) Ta/NiFe/PdPtMn (15)/CoFeB (1.5)/Ru (0.8)/CoFeB (2.5)/Cu (2.8) /CoFeB (4)/Cu (2.8)/CoFeB (2.5)/Ru (0.8)/CoFeB (1.5)/PdPtMn (15) and 2) Ta/NiFe/PdPtMn (15)/CoFeB (4)/Ru (0.8)/CoFeB (5)/Cu (5)/CoFeB (7)/Cu (5)/CoFeB (5)/Ru (0.8)/CoFeB (4)/PdPtMn (15). The CPP GMR properties of all of these SV films are shown in **Figure 6**. The Δ*RA* values of the single and dual types with thicker magnetic layers were larger than the Δ*RA* values of the thinner types. Also, the dual type SV showed a larger Δ*RA* because the SV structure has four magnetic/non-magnetic layer surfaces. The *RA* and Δ*RA* of the dual type SV with thicker magnetic layers were 130 mΩμm^2 and 2.25 mΩμm^2, respectively, and its MR ratio was 1.7% higher than the MR ratio of the dual type SV with the thinner magnetic layers. It should be mentioned that the Δ*RA* of the thick-type dual SV was four times higher than that of the thin-type single SV and this increase was due to the enhancements of bulk and interfacial scatterings caused by the increase in thickness of the magnetic layers and the magnetic/non-magnetic layer interfaces.

We applied the two-current series resistor model[4] to the SV-CPP elements because it assumes that the spin diffusion length is larger than the thickness of each layer, which was the case

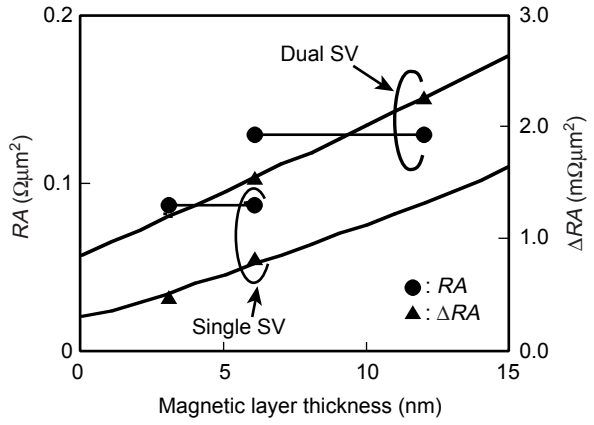

Figure 6
Total magnetic layer thickness dependence of *RA* and Δ*RA*. Solid lines are fitted to the two-current series resistor model.

with the SVs in this study. The model contains bulk scattering and interface scattering terms. We used the bulk resistivity and interface resistances that have been reported elsewhere[11] and a CoFeB bulk resistivity of 30 μΩcm, which was our experimentally measured value. When the bulk spin-asymmetry coefficient β equals 0.56 and the interface spin-asymmetry coefficient γ equals 0.75, there are good fits between the modeling results and the measured data. In the CPP mode, the bulk scattering term is important as well as the interface scattering term.

2.2.3 SV films with oxide layers

Even for the dual SV films, the Δ*RA* remains at several mΩμm^2. Therefore, it is difficult to obtain sufficient output voltage from a conventional SV. To overcome this problem, we tried to enhance the Δ*RA* by inserting oxide layers in the SV films. Except for the oxide layers, the stacking layers were the same as in the conventional single SV. During the deposition process, the pinned layer was oxidized by introducing oxygen gas into the chamber. The top layer of Ta was also oxidized in-situ after deposition by exposing it to oxygen plasma. The exposure duration was between 30 s and 200 s. An additional Cu capping layer was sequentially deposited in the same sputtering machine.

Figure 7 shows the *RA* and Δ*RA* as a functions of the oxidization time. The *RA* and Δ*RA* increased as the exposure time was increased up to 100 s. At 100 s, the Δ*RA* reached 9.0 mΩμm^2, which is about 25 times larger than that of the conventional single SV element. The increase in Δ*RA* in the intermediate oxidization time (100 s) suggests that the enhancement of Δ*RA* was partially due to the microscopically inhomogeneous current flow through the oxide layers, which makes current flow inhomogeneous in free/Cu/pinned layers and leads to an enhanced resistance change. In other words, the sensor element's effective size becomes smaller than its physical dimensions.

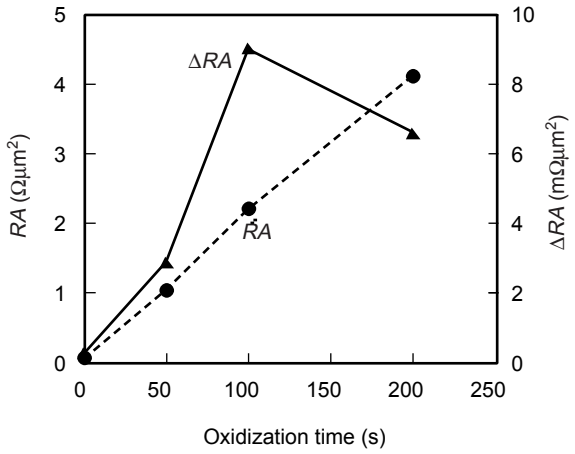

Figure 7
RA and Δ*RA* of a single SV with an oxide layer.

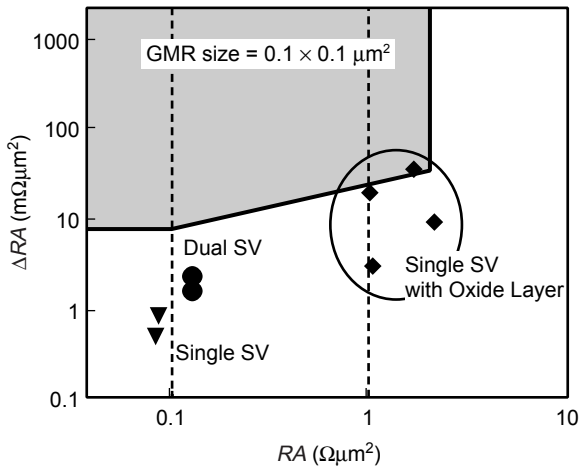

Figure 8
Δ*RA* vs. *RA* of SV films.

Figure 8 shows the Δ*RA* vs. *RA* of these SV films. Recently, we fabricated two types of single SV films with an oxide layer. The *RA* and Δ*RA* values were, respectively, 1 Ωμm² and 18.9 mΩμm² for the first type and 1.7 Ωμm² and 34 mΩμm² for the second type. We have just started to estimate the reliability of these films at various current densities. So far, these films have proved to be reliable at a current density of 13 MA/cm². This is still not enough for use in a read head, so we need to modify the material and/or the method of forming the oxide layer. However, our results show that the target properties can be achieved by using a structure such as an oxide layer to control the flow of current.

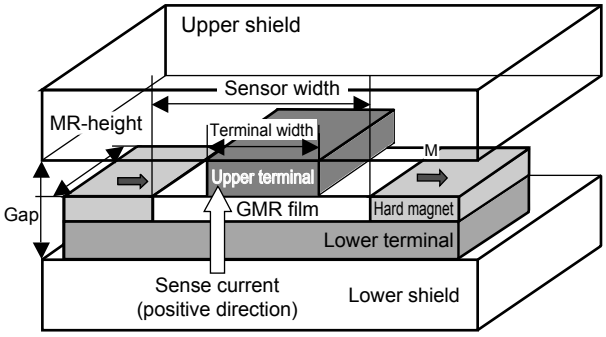

Figure 9
Model of CPP head.

Table 1
Conditions of CPP head simulation.

Parameters	Case I	Case II
RA (Ωμm²)	0.15	1.7
Δ*RA* (mΩμm²)	3.0	34
MR ratio (%)	2.0	2.0
Terminal width (μm)	0.1	
Sensor width (μm)	0.18	
MR height (μm)	0.1	
MR resistance (Ω)	13.2	165.0
Free layer tBs (T nm)	3.1	
Medium tBr (T nm)	3.5	
Write track width (μm)	0.2	
Magnetic space (nm)	18	
Power consumption (mW)	0.55	
Sense current (mA)	6.4	1.8

2.3 Simulation of head performance

2.3.1 Simulation model

In parallel with the experiments discussed above, we have designed a new CPP head and studied its read-back performance using a micromagnetics simulator. The model of the head viewed from the air bearing surface (ABS) is shown in **Figure 9**, and the model's parameters are listed in **Table 1**. For this head, we say that the direction of I_s is positive when it creates a magnetic field in the same direction as the field of the hard magnets at the ABS. I_s is positive in this head when it flows from the lower shield to the upper shield. The upper terminal's width and height are both 0.1 μm, and the sensor width is

Table 2
Results of simulations.

	Case I	Case II
Read-back voltage (μVp-p)		
Positive direction (I_s+)	255	845
Negative direction (I_s-)	308	897
Effective core width (μm)		
Positive direction (I_s+)	0.152	0.124
Negative direction (I_s-)	0.133	0.117
Head SNR (dB)		
Positive direction (I_s+)	20.7	20.1
Negative direction (I_s-)	22.3	20.6

0.18 μm. In this model, the sensitivity profile of the sensor is determined mainly by the terminal width. This structure does not have the problem of diffusive electron scattering at the edges of the GMR pillars.[12] The head's properties were calculated for two common applications of CPP elements: a low-impedance sensor in a conventional SV (Case I) and a moderate-impedance sensor equivalent to an SV with an oxide layer (Case II). For Case I, RA and ΔRA were assumed to be 0.15 Ωμm^2 and 3.0 mΩμm^2, respectively. For Case II, we used 1.7 Ωμm^2 for RA and 34 mΩμm^2 for ΔRA, which are measured values obtained through experiment. The MR ratios were 2% for both cases. The limit of the power consumption P determines the amplitude of the head's I_s. According to simple thermal analysis, P = 0.55 mW leads to a temperature rise of 30 degrees in the CPP-head structure. Therefore, we assumed that P = 0.55 mW in all of the simulations. The I_s distribution was determined, and then the magnetic field induced by the I_s was calculated.

2.3.2 Simulation results and discussion

The results of the simulation are listed in **Table 2**. The crosstalk was calculated for a track pitch of 0.23 μm and a write track width of 0.2 μm. The center track was 490 kFCI, and the neighboring side-tracks were 32 kFCI. Due to the constant P, the higher resistance head (Case II) has a higher read-back signal. This is because $P = I_s^2 R$ and, since the output voltage is approximately proportional to $I_s R$, it is therefore approximately proportional to $(PR)^{1/2}$. In Case II, the peak-to-peak read-back voltage is 845 μV at a positive sense current of 1.8 mA.

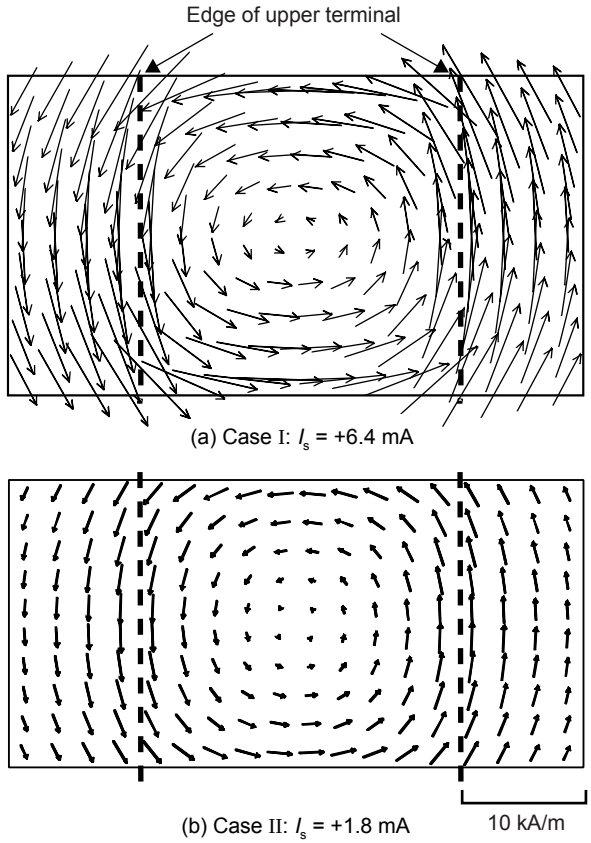

Note) The lengths of the arrows are proportional to the magnitude of the in-plane magnetic field.

Figure 10
In-plane magnetic field induced by the sense current at the free layer.

The magnetic field induced by the sense current greatly affects the read-back performance. In Case I, the sense current was 6.4 mA and the magnetic field created by the sense current was calculated to be about 8 kA/m at the ABS, while a negative sense current cancels the magnetic field from the hard magnets. This is probably the reason why a higher output voltage is obtained in the negative sense-current case. The effective read core-width is also narrower than that in the positive current case for the same reason. However, from the viewpoint of operation stability, a positive current is preferable. **Figure 10** shows the distribution of the magnetic field created by the

sense-current in the free layer for each case. The sensor, which has moderate impedance in Case II, is more practical because the magnitude and distribution of the magnetic field are smaller than in Case I.

Figure 11 shows the micro track profiles of the CPP heads in the positive direction of I_s. The profiles were calculated for a 0.01 μm-width micro-track. The effective core width of Case II is smaller than that of Case I. This is due to the different current distribution between both heads. The larger resistance of the element compared with that of the terminal makes the distribution of the sense current uniform. Therefore, in Case I, the distribution of current density is larger than in Case II and its current density near the edge of the current terminal is much higher than in the center.

Simulation studies revealed that a conventional SV CPP head with a 0.1 μm-width and 0.1 μm-height has too low an impedance and a large magnetic field induced by the sense current, which greatly affect the read-back performance. Moreover, our model shows that the sense current is concentrated at the edge of the terminal, which will increase the read core width.

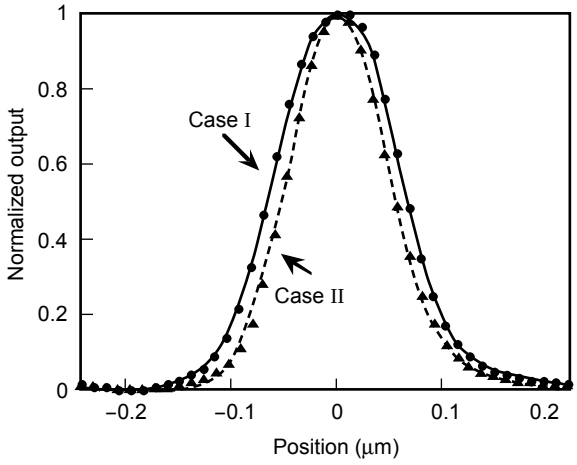

Figure 11
Micro track profiles of the CPP heads.

2.3.3 Signal-to-noise ratio estimation

Lastly, we estimated the signal-to-noise ratio of our new SV-CPP head. The conditions assumed for the estimation are shown in **Table 3**. The rms voltage of the high-frequency signal S_{Hf} was assumed to be about 55% of the value for the low-frequency signal S_{Lf} which was simulated as described above. The total noise N_T includes the head, medium, and circuit noises. The head noise increases proportionally with the square root of the resistance of the element, and the medium noise increases proportionally with the signal. The signal-to-noise ratios (S_{Hf}/N_T) of Cases I and II, which both had MR ratios of 2%, were estimated to be 8.6 dB and 13.6 dB, respectively (**Figure 12**). Case II showed a higher S_{Hf}/N_T than Case I, in spite of its larger head and medium noises. How-

Table 3
Conditions for signal-to-noise ratio estimation.

MR height	0.1 μm
Core width	0.1 μm
Power consumption	550 μW
Temperature	300 K
Bandwidth	230 MHz
Resolution of S_{Hf}	55%
Circuit noise	16 μVrms
S_{Lf}/N-medium	25 dB

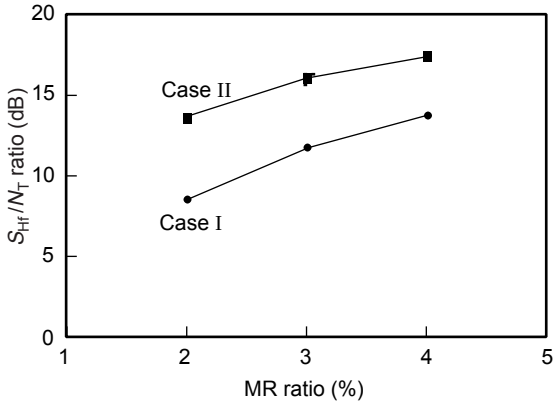

Figure 12
Results of signal-to-noise ratio estimation.

ever, the S_{Hf}/N_T of Case II is still low. An element with an MR ratio of about 4% would have an S_{Hf}/N_T as high as 17.3 dB, which is sufficient for a recording system.

CPP heads with moderate impedance show several advantages compared with low-impedance CPP heads, for example, a higher output voltage, larger signal-to-noise ratio, less influence from the magnetic field induced by the sense-current, macroscopically uniform current distribution throughout the sensor, and a narrower read core width.

3. Conclusion

We have investigated and improved the MR properties of the SV in the CPP mode for applications in read heads. The conventional single SV film shows an RA of 100 mΩμm^2 and a ΔRA of 0.59 mΩμm^2. However, a single SV with an oxide layer drastically increased RA to 1.7 Ωμm^2 and ΔRA to 34 mΩμm^2. We think that this enhancement is partially due to the microscopic inhomogeneous current-flow through the oxide layer, which leads to a narrower effective current flow area.

Simulation studies showed the advantage of moderate-impedance sensors compared with low-impedance sensors, for example, a higher output voltage, higher signal-to-noise ratio, less influence by the magnetic field induced by the sense current, microscopically uniform current distribution throughout the sensor, and a narrower read core width. When the sensor size is 0.1 μm × 0.1 μm, which corresponds to a 100 Gbit/in^2 level head, and RA = 1.7 Ωμm^2 and ΔRA = 34 mΩμm^2, a peak-to-peak read-back voltage of 845 μV was obtained with P = 0.55 mW.

Our results show that the target properties for an over 100 Gbit/in^2 read sensor can be achieved with a CPP-SV that is given an oxide layer to increase the resistance change and control the resistance. We therefore believe that the CPP-SV head will play an important role in the read heads of future HDDs.

References

1) W. P. Pratt Jr., S. F. Lee, J. M. Slaughter, R. Loloee, P. A. Schroeder, and J. Bass: Perpendicular giant magnetoresistances of Ag/Co multilayers. *Phys. Rev. Lett.*, **66**, p.3060-3063 (1991).
2) S. Zhang and P. M. Levy: Conductivity perpendicular to the plane of multilayered structures. *J. Appl. Phys.*, **69**, p.4786-4788 (1991).
3) G. E. W. Bauer: Perpendicular transport through magnetic multilayers. *Phys. Rev. Lett.*, **69**, p.1676-1679 (1992).
4) T. Valet and A. Fert: Theory of the perpendicular magnetoresistance in magnetic multilayers. *Phys. Rev. B*, **48**, p.7099-7113 (1993).
5) A. Vedyayev, M. Chshiev, N. Ryzhanova, B. Dieny, C. Cowache, and F. Brouers: A unified theory of CIP and CPP giant magnetoresistance in magnetic sandwiches. *J. Magn. Magn. Mater.*, **172**, p.53-60 (1997).
6) W. H. Butler, X. -G. Zhang, and J. M. MacLaren: Solution to the Bolzmann equation for layered systems for current perpendicular to the planes. *J. Appl. Phys.*, **87**, p.5173-5175 (2000).
7) R. Rottmayer and J. -G. Zhu: A new design for an ultra-high density magnetic recording head using a GMR sensor in the CPP mode. *IEEE Trans. Magn.*, **31**, p.2597-2599 (1995).
8) J. P. Spallas, M. Mao, B. Law, F. Grabner, D. O'Kane, and C. Cerjan: Improved performance of Cu-Co CPP sensors. *IEEE Trans. Magn.*, **33**, p.3391-3393 (1997).
9) K. Nagasaka, Y. Seyama, L. Varga, Y. Shimizu, and A. Tanaka: Giant magnetoresistance properties of specular spin valve films in CPP structure. *J. Appl. Phys.*, **89**, p.6943-6945 (2001).
10) A.Tanaka, Y. Shimizu, H. Kishi, K. Nagasaka, H. Kanai, and M. Oshiki: Top, bottom, and dual spin valve recording heads with PdPtMn antiferromagnets. *IEEE Trans. Magn.*, **35**, p.700-705 (1999).
11) A. C. Relliy, W. Park, R. Slater, B. Ouaglal, R.

Loloee, W. P. Pratt Jr., and J. Bass: Perpendicular giant magnetoresistance of $Co_{91}Fe_9$/Cu exchange-biased spin-valves: further evidence for a unified picture. *J. Magn. Magn. Master.,* **195**, L269-L274 (1999).

12) B. Dieny, M. Li, S. Liao, and K. Ju: Effect of scattering at lateral edges on the current - perpendicular - to plane giant magnetoresistance of submicronic pillars. *J. Appl. Phys.*, **89**, p.7302-7304 (2001).

Keiichi Nagasaka received the B.S. and M.S. degrees in Materials and Science Engineering from Tohoku University, Miyagi, Japan in 1994 and 1996, respectively. He joined Fujitsu Laboratories Ltd., Atsugi, Japan in 1996, where he has been engaged in research and development of magnetic recording heads. He is a member of the Magnetic Society of Japan.

Yoshihiko Seyama received the B.S. degree in Physics from Chiba University, Chiba, Japan in 1986. He joined Fujitsu Laboratories Ltd., Atsugi, Japan in 1986, where he has been engaged in research and development of magnetic recording heads. He is a member of the Magnetic Society of Japan.

Reiko Kondo received the B.S. degree in Applied Physics from the Science University of Tokyo, Tokyo, Japan in 1988. She was a Visiting Scientist at Stanford University, California, USA from 1995 to 1996. She joined Fujitsu Laboratories Ltd., Atsugi, Japan in 1997, where she has been engaged in research and development of magnetic recording heads. She is a member of the Magnetic Society of Japan.

Hirotaka Oshima received the B.S., M.S., and Ph.D degrees in Applied Physics from the University of Tokyo, Tokyo, Japan in 1996, 1998, and 2001, respectively. He joined Fujitsu Laboratories Ltd., Atsugi, Japan in 2001, where he has been engaged in research and development of magnetic recording read heads. He is a member of the Physical Society of Japan.

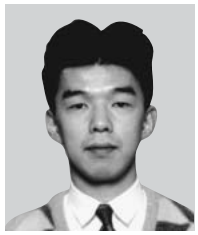

Yutaka Shimizu received the B.S. and M.S. degrees in Materials and Science Engineering from Waseda University, Tokyo, Japan in 1988 and 1990, respectively. He joined Fujitsu Laboratories Ltd., Atsugi, Japan in 1990, where he has been engaged in research and development of magnetic recording heads. He is a member of the Magnetic Society of Japan.

Atsushi Tanaka received the B.S. and M.S. degrees in Applied Physics from the University of Tokyo, Tokyo, Japan in 1979 and 1981, respectively. He joined Fujitsu Laboratories Ltd., Atsugi, Japan in 1985, where he has been engaged in research and development of magnetic materials and recording heads. He is a member of the Magnetic Society of Japan and the Japan Society of Applied Physics.